

# Multiple micro-optical atom traps with a spherically aberrated laser beam

P Ahmadi<sup>†</sup>, V Ramareddy and G S Summy

Department of Physics, Oklahoma State University, Stillwater, Oklahoma 74078-3072

**Abstract.** We report on the loading of atoms contained in a magneto-optic trap into multiple optical traps formed within the focused beam of a CO<sub>2</sub> laser. We show that under certain circumstances it is possible to create a linear array of dipole traps with well separated maxima. This is achieved by focusing the laser beam through lenses uncorrected for spherical aberration. We demonstrate that the separation between the micro-traps can be varied, a property which may be useful in experiments which require the creation of entanglement between atoms in different micro-traps. We suggest other experiments where an array of these traps could be useful.

PACS numbers:

Submitted to: *New J. Phys.*

<sup>†</sup> To whom correspondence should be addressed (peyman@okstate.edu)

## 1. Introduction

The trapping of atoms at the intensity maximum of an optical field that is far-detuned to the red of an atomic transition has been the subject of study for almost a decade now [1, 2]. There has been a rapid growth of interest in these far-off resonant optical traps (FORTs) because of their versatility and wide range of possible applications. For example, they have been used to create an all optical Bose-Einstein condensate [3, 4, 5], a degenerate Fermi gas [6] and an all optical atomic laser [7]. These traps in the form of optical lattices have been employed in theoretical models to open new frontiers in quantum information research. The proposal of Brennen *et al.* [8] for quantum logic gates using neutral atoms in optical lattices, provided a way around the decoherence problem which affects schemes involving charged particles. They showed that entanglement between a collection of trapped neutral atoms can be created with a laser using the induced electric dipole-dipole interaction. The main difficulty associated with their scheme has been the need to construct a lattice FORT with sufficient separation between unit cells to address them individually and with a sufficient volume to load many atoms at each trapping site. These challenges have been the focus of another series of experimental efforts. For example, using a holographic phase plate, Boiron *et al.* [9] constructed an optical lattice with a period of  $29\mu\text{m}$  using a YAG laser. In other experiments, the Hannover group have developed a technique using arrays of microlenses to focus a red detuned laser beam and create a series of micro-traps for use as quantum memories [10, 11, 12]. Peil *et al.* [13] employed two independent optical lattices, whose spatial periods differ by a factor of three, to load a Bose-Einstein condensate of Rb 87 atoms in sites having a separation approximately  $30\mu\text{m}$ .

In most FORT experiments atoms are trapped at the intensity maxima formed by a focused laser beam in either a travelling or standing wave configuration. In this paper, we demonstrate a new approach in which the peaks in the diffraction pattern associated with spherical aberration in the vicinity of the focal plane of a lens are used to create a linear array of micro-traps. The primary spherical aberration pattern close to the focal plane has been studied and well documented by several authors. For example, Evans and Morgan [14, 15] theoretically produced the aberration pattern of a lens that was not corrected for spherical aberration in order to explain laser induced breakdown in gases, while Smith [16] experimentally verified the primary spherical aberration intensity distribution produced by a lens uncorrected for spherical aberration. The spherical aberration in our experiments is induced by the lenses in the path of a  $\text{CO}_2$  laser beam. It will be seen that most of the contribution to the spherical aberration comes from the final lens (primary lens) which is employed to focus the  $\text{CO}_2$  laser beam onto a cold atomic cloud. We will show that varying the incident beam size on the primary lens enables us to change the aberration pattern and hence control the separation of the micro-traps over a range of about a millimeter. One of the advantages of our set up is the use of a  $\text{CO}_2$  laser as a far off-resonant light source. This considerably improves the coherence time compared to some of the atom optical experiments mentioned above

which use YAG lasers to create dipole traps with micron size separation. Furthermore, the ability to vary the spacing between the micro-traps over a range of about a millimeter makes the addressing of the individual traps feasible using the techniques developed by Nägerl *et al.* [17].

This paper is constructed as follows. In section 2 we discuss the theory of the multiple trap potential that is used in simulations. Section 3 is devoted to the description of the experimental setup. In section 4 we present the experimental data and compare them with our simulation results. Our suggestions and future plans for the use of these potentials appear in the conclusion section.

## 2. Aberration effect of a lens on the incident laser light near the focus

Since the potential well depth of any FORT is proportional to the intensity, we now proceed to calculate the intensity distribution produced near the focus of the lens used in our experiment. Following Born and Wolf [18] and Yoshida and Asakura [19], the intensity close to the focus of a lens for an incident Gaussian beam is given by,

$$I(u, v) = \frac{1}{w^2} \left| \int_0^1 \rho \, d\rho \, e^{\frac{-\rho^2}{(w/a)^2}} e^{-i\left(\frac{u\rho^2}{2} + k\beta\rho^4\right)} J_0(v\rho) \right|^2, \quad (1)$$

where  $w$  is the spot size on the lens and  $\rho$  is the radial coordinate on the lens normalized to the radius of the lens,  $a$ .  $v$  and  $u$  are the scaled cylindrical radial and axial coordinates of the image space (with the origin for  $u$  at the Gaussian focus) and are given by  $v = \frac{2\pi}{\lambda} \frac{a}{R} \sqrt{x^2 + y^2}$  and  $u = \frac{2\pi}{\lambda} \left(\frac{a}{R}\right)^2 z$ .  $k$  is the vacuum wave number, given by  $k = 2\pi/\lambda$ , where  $\lambda$  is the wavelength of the light used.  $R$  is the radius of the Gaussian reference sphere from the lens,  $(x, y)$  are the cartesian coordinates in the Gaussian image plane and  $\beta$  is the primary spherical aberration coefficient, usually expressed in terms of the number of wavelengths. This coefficient is additive over all the elements used in an optical system. Our set up has three lenses in the path of the laser light (see Fig. 1). The first two lenses constitute a telescope and the third one (which is placed inside the vacuum chamber) we refer to as the primary lens.

Using the thin lens approximation, we calculate the primary spherical aberration produced by such a lens of focal length  $f$  to be [20],

$$\beta = \frac{w^4}{32f^3} \left[ \left(\frac{n}{n-1}\right)^2 + \frac{(n+2)}{n(n-1)^2} \left(B + \frac{2(n^2-1)}{n+2}C\right)^2 - \frac{n}{n+2}C^2 \right], \quad (2)$$

where  $n$  is the refractive index of the lens medium and  $B$  is the shape variable given by  $B = (c_1 + c_2)/(c_1 - c_2)$  and  $c_i = 1/r_i$ ;  $i = 1, 2$ ;  $r_i$  are the radii of curvature of the lens surfaces.  $C$  is known as the conjugate variable and is defined as  $C = (u_1 + u_2)/(u_1 - u_2)$ , where  $u_1$  and  $u_2$  are the divergence angles of the gaussian beam before and after passing through the lens. These angles are given by  $u_i = \lambda/\pi w_{0i}$ ;  $i = 1, 2$ , where  $w_{01}$  and  $w_{02}$  are the minimum beam waists of the beam before and after the lens. It should be noted that according to the usual sign convention, if the lens produces a converging beam,

then  $u_2$  is negative so that the denominator in the definition of  $C$  is not zero in our experiment.

In the experimental situation we wish to model, the separation of the telescope lenses is varied by moving the second lens in the optical system and keeping the other lenses fixed. Thus the first lens of the telescope contributes a constant amount to the total spherical aberration coefficient  $\beta$  as its  $w$  and  $C$  parameters are fixed. As the position of the second lens in the telescope is moved, the beam size on this lens and on the third (the primary) lens will change resulting in changes to the parameters  $w$  and  $C$  for these lenses. This leads to a variable contribution to  $\beta$  by these last two lenses and therefore a variable aberration pattern near the focus of the primary lens. We have found that for our experiment the primary spherical aberration of the primary lens varies from around 0.1 up to around 18.2 wavelengths.

### 3. Experimental set up

In the following, we present an experimental setup which enables us to create the spherical aberration pattern to form a series of micro optical traps. Our experimental apparatus consists of a stainless steel, octagonal vacuum chamber which is maintained at a pressure of approximately  $5 \times 10^{-10}$  torr by an ion pump. A 3.1 cm diameter ZnSe viewport allows us to focus the  $10.6 \mu\text{m}$  light from a  $\text{CO}_2$  laser into the center of this chamber. The focusing lens (the primary lens) is a meniscus lens with a 3.81 cm focal length and 2.54 cm diameter placed inside the vacuum chamber and is not corrected for spherical aberration<sup>†</sup>. This lens is mounted such that the convex side is towards the center of the chamber to maximize the spherical aberration effects. Before reaching the primary lens, the  $\text{CO}_2$  laser beam passes through a telescope composed of two plano convex lenses with 6.35 cm and 12.7 cm focal lengths placed approximately 2 meters away from the chamber. This configuration allows us to control the beam size at the lens inside the chamber by varying the separation of the telescope lenses. Consequently, we are able to change the spherical aberration pattern close to the gaussian focus inside the chamber.

The trapping light was directed into the vacuum system in a geometry such that it propagated at an angle of 45 degrees to the vertical. The light for this beam originated from a 50 Watt, RF excited  $\text{CO}_2$  laser. The total laser power was controlled by passing the output light through an acousto-optic modulator (AOM). The first order of the modulator was then directed into the telescope to expand the beam. The optical arrangement used in this experiment is as shown in Fig.1. For our atomic source we used a magneto-optic trap (MOT), formed with a 20 G/cm magnetic field gradient, and by two 5 cm diameter, 20 mW beams. Each beam made three passes through the chamber and was detuned 15 MHz below the  $F = 2 \rightarrow F' = 3$  transition of the D2 line of Rb 87. Repumping light tuned to the  $F = 1 \rightarrow F' = 2$  transition propagated with one of the trapping beams. We were able to capture about  $2 \times 10^7$  atoms with

<sup>†</sup> Note that for some of the later experiments, this lens was replaced by an aspheric lens

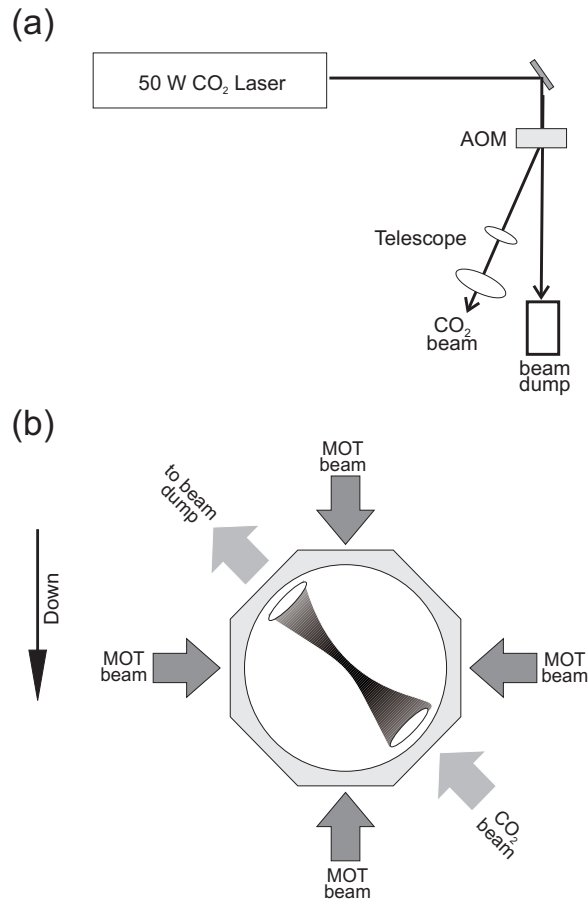


**Figure 1.** Experiment schematic, showing (a) the production of the FORT beams and its path before it enters the chamber, and (b) the beam geometry relative to the vacuum chamber.

this arrangement. One of the most difficult aspects involved in the setup of a FORT is the beam alignment. Since the FORT light is so far from resonance, no fluorescence is induced and it is hard to determine whether the FORT beam is overlapping with the MOT or not. To overcome this difficulty we have devised a method which allows us to observe the position of the CO<sub>2</sub> laser beam in real time directly on an inexpensive CCD camera that normally monitors the MOT. To accomplish this it is necessary to improve the contrast between the atoms trapped in the MOT and those trapped in the FORT. Several techniques will work, for example, increasing the detuning of the MOT light from resonance, or reducing the intensity of the MOT light. A similar effect is obtained if these operations are performed on the repumping light. With any one of these methods, the brightness of the MOT and the effect of its near resonant light on pushing atoms out of the FORT, can be lessened. However, there can still be enough near-resonant light present in the MOT beams to cause atoms that are contained in the FORT to fluoresce and hence make the FORT beam visible. Using these techniques greatly simplifies alignment of our CO<sub>2</sub> laser beam, turning a task which could previously take several days into one that can be performed in minutes.

To load the FORT with atoms we apply the following procedure. First the MOT is loaded for 30 seconds from the background vapor while at the same time the CO<sub>2</sub> laser remains switched on. Then, as a key step in efficiently loading the FORT, we reduce the repump intensity by a factor of 50 compared to its initial value to make a temporal dark SPOT [21, 22]. This strong reduction in the repump power occurs 50 to 70 ms before switching off the MOT trapping beams. Alongside reducing the repump power, we jump the trapping beam detuning to  $-80$  MHz for further laser cooling and to counteract the detuning change induced by the light shift of the CO<sub>2</sub> beam. If we did not jump the detuning, atoms in the region of the FORT would see the MOT beams positively detuned, thus reducing the effectiveness of the MOT. Finally, after the main MOT beams have been extinguished, we adiabatically switch off the MOT magnetic field. The earliest time that we can image the FORT is 100 ms after releasing the MOT. This ensures that any of the untrapped atoms have sufficient time to fall away from the FORT under the influence of gravity. Both the MOT and the FORT are destructively imaged by observing the absorption of a resonant probe laser which passes through the atom cloud and is incident on a CCD camera. By integrating the optical density across the atom cloud we are able to determine the number of trapped atoms. When imaging the FORT, the CO<sub>2</sub> laser beams are switched off 3.5 ms before the image is taken to allow the cloud of atoms to expand to a size which is significantly above the resolution of the optical system.

#### 4. Results and Discussion

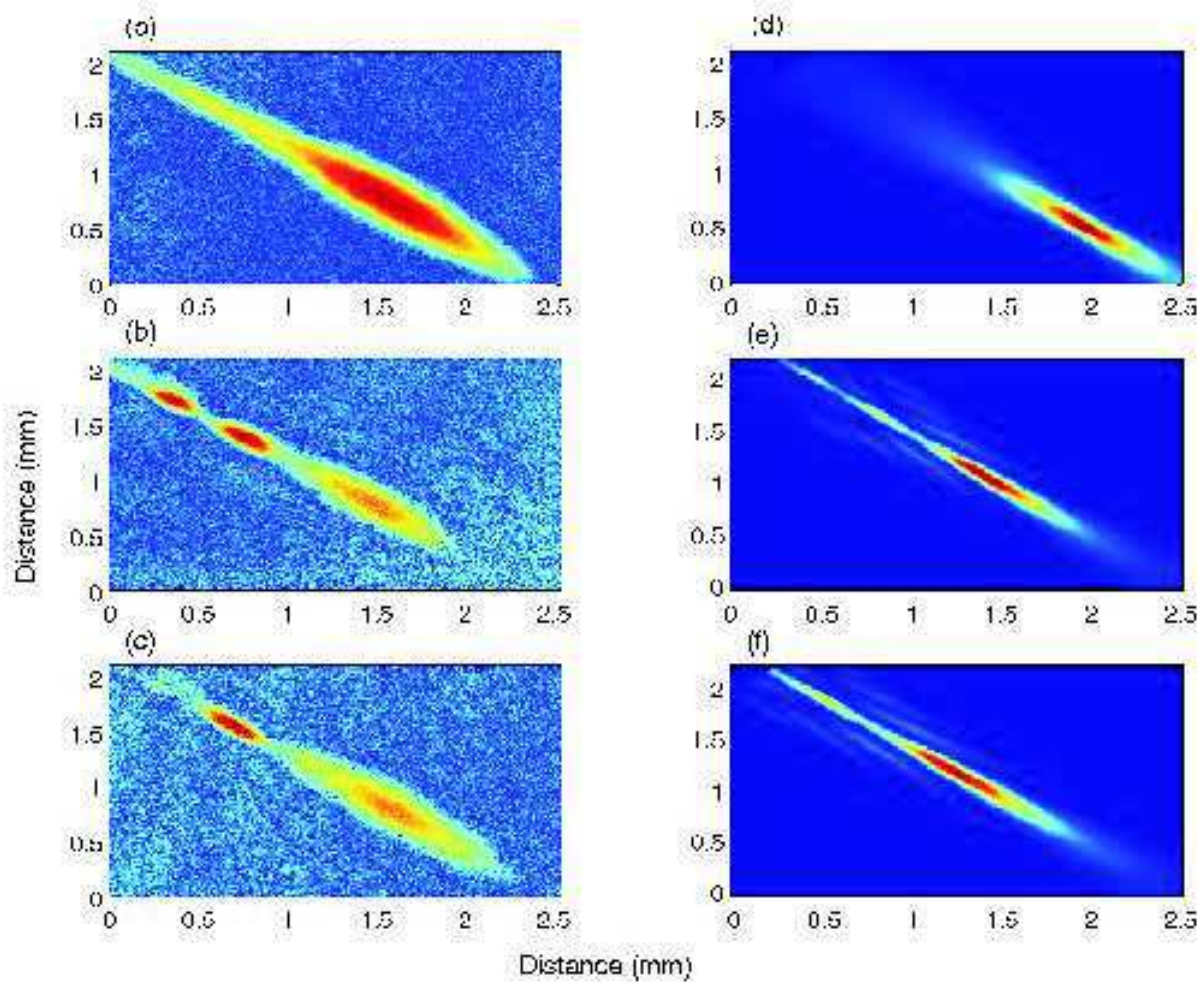
Using the procedure described in Section 3 we have been able to load several micro-optical traps created by the aberration pattern of the meniscus lens. Interestingly, our observations show that there are approximately 10 sites capable of holding the atoms when the beam diameter is similar to the size of the primary lens, in very good agreement with our simulation results. For a given amount of spherical aberration  $\beta$ , the separation between the micro-traps decreases as one moves away from the focus and towards the primary lens. Therefore the number of micro-traps being loaded from a MOT at a given time depends where the MOT and FORT overlap each other. Usually 3 micro-traps are loaded by placing the atomic cloud of the the MOT close to the gaussian focus of the lens. This can be increased to 4 or 5 micro-traps by moving the MOT a few millimeters towards the lens (to move the MOT we change the currents in the nulling coils designed to cancel out stray magnetic fields). Fig. 2 shows three absorption images of the FORT and their corresponding simulated potentials at two extreme separations of the telescope lenses and one intermediate separation. The lower panel of Fig. 2 shows that the central FORT and one micro-trap are loaded. This happens when there is higher spherical aberration  $\beta$ . Our simulations show that the separation between the peaks is greater when there is a high spherical aberration. So in the lower panel of Fig. 2, the spacial extent of the MOT is such that it could load only one micro-trap along with the central FORT. For the parameters of Fig. 2(c), we found from equation 2 that the

spherical aberration  $\beta$  is around 18.2 wavelengths. The central panel of Fig. 2 shows the central FORT and two micro-traps that are loaded when  $\beta$  is around 12.6 wavelengths. In the upper picture, the spherical aberration is diminished by the small beam size on the primary lens so that only the highly populated central FORT remains. This higher population is due to the fact that for such cases the beam is not focused tightly so that the capture volume of the FORT is increased. In the absence of the spherical aberration the central FORT usually contains  $10^6$  trapped atoms. In the presence of the spherical aberration, the other micro-traps usually have  $2 \times 10^5$  atoms at  $70\mu\text{K}$  temperature.

According to our numerical simulations, the spherical aberration contributions from the telescope lenses can also alter the intensity pattern close to the focal plane of the primary lens. Our telescope lenses are not corrected for the spherical aberration. To demonstrate this point the meniscus lens was replaced with an aspheric lens corrected for spherical aberrations so that the primary lens did not alter the wave front because of the spherical aberration. Different combinations of lenses that made up the telescope were tested, however all of them showed a similar pattern. Thus, here we shall present only one set up in which we used two plano convex lenses, both with 12.7cm focal length. The separation of the telescope lenses was initially set equal to 24cm and was then decreased in 3mm steps. Fig. 3 shows the observed intensities along the optical axis of the primary lens as the telescope separation was varied. An offset has been added to each profile to improve the readability. The sequence from the top is in order of increasing distance between the telescope lenses. This figure shows that a micro trap is created from the central FORT and starts to move away from it as we increase the separation of the telescope lenses. This is because as the beam size on the second lens increases so does the spherical aberration. From Fig. 3 it can be noted that after the seventh step of increment in the telescope separation a second micro-trap emerges from the central FORT and moves away. This happens while the first micro-trap has travelled far enough so that atoms are no longer loaded into it. The second micro-trap moves away with increasing telescope lens separation until the fifteenth step when a third micro-trap emerges from the central trap and starts to travel towards the second micro-trap. These two micro-traps coexist for a few more increments in the separation until the second micro-trap fails to load atoms. Since less atoms are loaded into the micro-traps of Fig. 3 compared to Fig. 2, we infer that the meniscus lens produces more spherical aberration than the telescope lenses.

## 5. Conclusion

We have shown that the intensity distribution produced by a lens that is not corrected for spherical aberration can be used to prepare a potential to realize micro-optical traps. A beam from a  $\text{CO}_2$  laser focused with such a lens was employed to load Rb 87 atoms into the micro-optical traps formed by the intensity maxima of the spherical aberration pattern. Such high density ( $10^{13}$  atoms/cm<sup>3</sup>) samples of cold atoms are of interest for a wide range of experimental studies including evaporative cooling, cold collisions





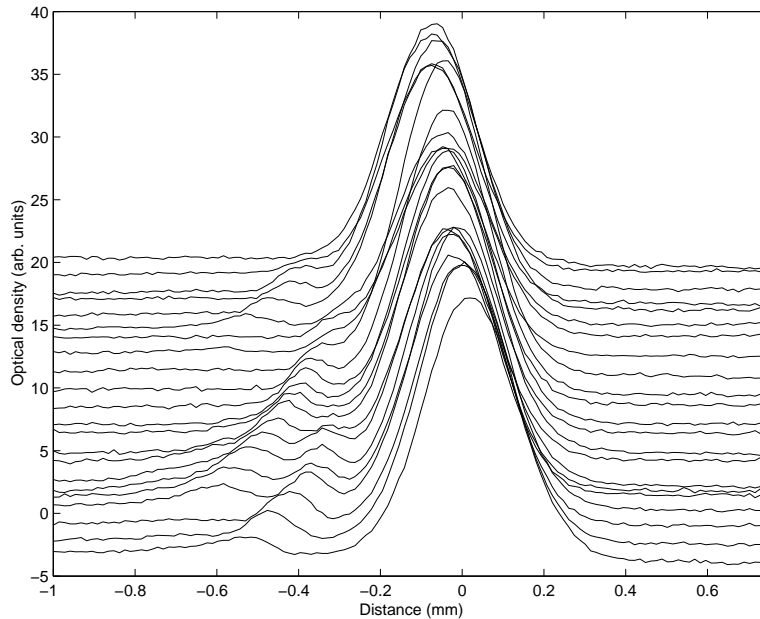


**Figure 3.** Experimentally observed intensity integrated perpendicular to the optical axis when the aberration is only due to the telescope lenses. Each curve is for various telescope lens separations.

and quantum information processing with ultra cold Rydberg atoms [23]. Furthermore, the variable separation of the micro-traps could be used to control the dipole-dipole interactions between the atoms in adjacent trapping sites. Also increasing the separation of the micro-traps up to a few hundred microns makes the task of individually addressing the different micro-traps relatively straight forward with existing optical techniques. These properties are of great interest for quantum information processing proposals for neutral atoms. Another possible experiment would be to construct an atom interferometer using the micro-traps. One could take a BEC formed using evaporative cooling in a single focused laser beam [24] and then by changing the separation of the telescope lenses split off a sub group of BEC atoms. By simply setting the telescope separation back to the initial value the two BEC groups can be recombined making an interference pattern which depends on the phase difference accumulated between the wavefunctions. An analysis of such an interference pattern releases information about the mechanisms effecting the phase of the transported BEC. For example, if the second  $\text{CO}_2$  beam propagates in the vertical direction a phase will be induced to the wavefunction proportional to the change in the gravitational potential of the moving group. Therefore the final interference pattern contains information that could be used to probe gravity.

## 6. Acknowledgements

We wish to acknowledge Brian Timmons for his contributions to the experimental set up.

## References

- [1] C.S. Adams, H.J. Lee, N. Davidson, M. Kasevich, and S. Chu, Phys. Rev. Lett. **74**, 3577 (1995).
- [2] S. Friebe, C. D'Andrea, J. Walz, M. Weitz, and T.W. Hänsch, Phys. Rev. A **57**, R20 (1998).
- [3] M.D. Barrett, J.A. Sauer, and M.S. Chapman, Phys. Rev. Lett. **87**, 010404 (2001).
- [4] T. Weber, J. Herbig, M. Mark, H.C. Nägerl and R. Grimm, Science **299**, 232 (2003).
- [5] Y. Takasu, K. Maki, K. Komori, T. Takano, K. Honda, M. Kumakura, T. Yabuzaki, and Y. Takahashi, Phys. Rev. Lett. **91**, 040404 (2003).
- [6] S.R. Granade, M.E. Gehm, K.M. O'Hara, and J.E. Thomas, Phys. Rev. Lett. **88**, 120405 (2002).
- [7] G. Cennini, G. Ritt, C. Geckeler, and M. Weitz, Phys. Rev. Lett. **91** 240408 (2003).
- [8] G.K. Brennen, C.M. Caves, P.S. Jessen and I.H. Deutsch, Phys. Rev. Lett. **82**, 1060 (1999).
- [9] D. Boiron, A. Michaud, J.M. Fournier, L. Simard, M. Sprenger, G. Grynberg, and C. Salomon, Phys. Rev. A. **57**, R4106 (1998); R. Newell, J. Sebby, and T.G. Walker, Opt. Lett. **28**, 14, (2003).
- [10] R. Dumke, M. Volk, T. Mütter, F.B.J Buchkremer, G. Birkl, and W. Ertmer, Phys. Rev. Lett. **89**, 097903 (2002).
- [11] G. Birkl, F.B.J Buchkremer, R. Dumke, and W. Ertmer, Opt. Commun. **191**, 67 (2001).
- [12] F.B.J Buchkremer, *et al.*, Laser Phys. **12**, 736 (2002).
- [13] S. Peil, J.V. Porto, B.L. Tolra, J.M. Obrecht, B.E. King, M. Subbotin, S.L. Rolston and W.D. Phillips, Phys. Rev. A, **67**, 051603, (2003).
- [14] L.R. Evans and C.G. Morgan, Nature, **219**, 712, (1968).
- [15] L.R. Evans and C.G. Morgan, Phys. Rev. Lett. **22**, 1099, (1969).
- [16] L.M. Smith, J. Opt. Soc. Am. A., **6**, 1049 (1989)
- [17] H.C. Nägerl, D. Leibfried, H. Rohde, G. Thalhammer, J. Eschner, F. Schmidt-Kaler, and R. Blatt, Phys. Rev. A, **60**, 145 (1999).
- [18] M. Born and E. Wolf, "Principles of optics", 7 ed., p.519, 'Cambridge University Press' (1999).
- [19] A. Yoshida and T. Asakura, Opt. Comm. **25**, 133 (1978).
- [20] W.T. Welford, "Aberrations of the symmetrical optical system", p.192, 'Academic Press', London (1974).
- [21] S.J.M. Kuppens, K.L. Corwin, K.W. Miller, T.E. Chupp and C.E. Wieman, Phys. Rev. A, **62**, 013406 (2000).
- [22] W. Ketterle, K.B. Davis, M.A. Joffe, A. Martin and D.E. Pritchard, Phys. Rev. Lett. **70**, 2253 (1993).
- [23] M.D. Lukin, M. Fleischhauer, R. Cote, L.M. Duan, D. Jaksch, J.I. Cirac and P. Zoller, Phys. Rev. Lett. **87**, 037901 (2001).
- [24] We have recently realized an all optical BEC and successfully transferred it into the focus of a CO<sub>2</sub> laser beam. The details to be published elsewhere.